



Contents lists available at ScienceDirect

International Journal of Pharmaceutics

journal homepage: www.elsevier.com/locate/ijpharm



Duration of ultrasound-mediated enhanced plasma membrane permeability

Bart Lammertink^{a,*}, Roel Deckers^a, Gert Storm^{b,c}, Chrit Moonen^a, Clemens Bos^a

^a Imaging Division, University Medical Center Utrecht, Utrecht, Netherlands

^b Pharmaceutical Sciences, Utrecht University, Utrecht, Netherlands

^c Targeted Therapeutics, University of Twente, Enschede, Netherlands

ARTICLE INFO

Article history:

Received 6 October 2014

Received in revised form 8 December 2014

Accepted 9 December 2014

Available online xxx

Keywords:

Sonoporation

Ultrasound

Microbubbles

Drug delivery

Membrane permeabilization

Fluorescent model drug

ABSTRACT

Ultrasound (US) induced cavitation can be used to enhance the intracellular delivery of drugs by transiently increasing the cell membrane permeability. The duration of this increased permeability, termed temporal window, has not been fully elucidated. In this study, the temporal window was investigated systematically using an endothelial- and two breast cancer cell lines. Model drug uptake was measured as a function of time after sonication, in the presence of SonoVueTM microbubbles, in HUVEC, MDA-MB-468 and 4T1 cells. In addition, US pressure amplitude was varied in MDA-MB-468 cells to investigate its effect on the temporal window. Cell membrane permeability of HUVEC and MDA-MB-468 cells returned to control level within 1–2 h post-sonication, while 4T1 cells needed over 3 h. US pressure affected the number of cells with increased membrane permeability, as well as the temporal window in MDA-MB-468 cells. This study shows that the duration of increased membrane permeability differed between the cell lines and US pressures used here. However, all were consistently in the order of 1–3 h after sonication.

© 2014 Elsevier B.V. All rights reserved.

1. Introduction

Efficient and controlled drug delivery to tumor tissue remains one of the major challenges in pharmaceutical research. To achieve drug delivery to diseased tissue, drugs need to overcome several biological barriers. For drugs with intracellular targets, one of these barriers is the plasma membrane. Ultrasound (US) can be applied to overcome this barrier, improving cellular uptake of drugs and genes (Frenkel, 2008). US has been observed to increase, for example, the anti-tumor effectiveness of anticancer chemotherapeutics including bleomycin (Lamanauskas et al., 2013; Iwanaga et al., 2007), cisplatin (Sasaki et al., 2012; Heath et al., 2012), methotrexate (Mei et al., 2009) and gemcitabine (Kotopoulos et al., 2014), both *in vitro* and *in vivo*.

US has some major advantages over other intracellular drug delivery techniques, e.g., electroporation, since it can control

drug delivery non-invasively in a spatial and temporal manner (Deckers and Moonen, 2010). Microbubbles (MBs), initially developed as ultrasound contrast agents for diagnostic imaging, are now widely studied to enhance the effectiveness of therapeutic ultrasound (Hernot and Klivanov, 2008). MBs oscillate when exposed to US, and at low pressure amplitude, this can result in stable cavitation over a longer period of time. MB-mediated cavitation induces normal stresses and, through micro streaming, shear stresses to their environment. Higher pressure amplitudes may lead to inertial cavitation, in which the microbubbles collapse, and high velocity jets may occur (Kooiman et al., 2014). When in close proximity to cells, these effects can induce transient permeabilization of the plasma membrane (Van Wamel et al., 2006; Zhou et al., 2012), which, in turn, allows the intracellular delivery of non-permeant agents (Cavalli et al., 2013).

Plasma membrane permeabilization can be the result of oscillating microbubbles (Deng et al., 2004). Initially, this enhanced membrane permeability has been ascribed to pores in the membrane and was therefore termed sonoporation (Lentacker et al., 2014). Recently, it has been shown that these pores are not the only mechanism responsible for US induced drug uptake. Meijering et al. (2009) observed that endocytosis was up-regulated

* Corresponding author. Present address: UMC Utrecht, Heidelberglaan 100, Q00.3.11, Utrecht 3508 GA, Netherlands. Tel.: +31 88 75 696 65; fax: +31 88 75 558 50.

E-mail address: b.h.a.lammertink@umcutrecht.nl (B. Lammertink).

after US exposure and that the contribution of membrane pores and endocytosis to ultrasound induced uptake depended on the molecular size of the dye.

Another aspect of US induced membrane permeabilization under discussion, is the duration of increased cell membrane permeability, e.g., for hydrophilic low molecular weight drugs. This “temporal window” may influence future clinical protocols using sonoporation. The degree of US induced membrane damage leading to permeability has been reported to depend on exposure conditions, such as US pressure (Keyhani et al., 2001; Karshafian et al., 2009), duty cycle (Pan et al., 2005) and sonication time (Karshafian et al., 2009). To remain viable, cells need to recover from US induced plasma membrane damage. It has been shown that membrane pore resealing is influenced by pore size, ATP, extracellular $[Ca^{2+}]$ and presence of intracellular vesicles (Schlicher et al., 2006; Hu et al., 2013). Under normal physiological conditions *in vitro*, membrane recovery after US exposure was reported to take seconds (Mehier-Humbert et al., 2005; Zhou et al., 2009), minutes (Schlicher et al., 2006; Hu et al., 2013), or even hours (Zhao et al., 2008).

The duration of membrane permeability after sonication can also be measured by the internalization of a membrane impermeant model drug. A temporal window has been demonstrated in the order of seconds in bovine endothelial cells (Van Wamel et al., 2006), minutes in prostate cancer cells (Schlicher et al., 2006), or even 24 h in a glioma cell line (Yudina et al., 2011). These studies used similar small, hydrophilic dyes, i.e., propidium iodide (668 Da; Van Wamel et al., 2006), calcein (623 Da; Schlicher et al., 2006) and SYTOX[®] Green (600 Da; Yudina et al., 2011), all impermeable to viable cells. Since propidium iodide and SYTOX[®] Green are DNA intercalating agents, they are considered as model drugs for small hydrophilic chemotherapeutics, based on their physicochemical properties and target site.

Until now, no study, to our knowledge, reported the temporal window of different cell lines with identical experimental settings (i.e., US parameters, type of microbubble, model drug), and it remains unclear what causes the discrepancies in the reported temporal windows. Previous studies investigated the temporal window in either a cancer cell line or an endothelial cell line. Looking at future treatment strategies involving microbubbles and ultrasound, two routes of administration can be discriminated. The first involves intravenous administration of microbubbles and drugs, where US-activated microbubbles primarily affect endothelial cells. A second strategy implies intratumoral administration of microbubbles and drugs, where relative high local concentrations of MBs are in direct contact with tumor cells (Iwanaga et al., 2007; Matsuo et al., 2011; Watanabe et al., 2008).

From these perspectives, the objective of the present study was to investigate the temporal window of model drug uptake after US

exposure in an endothelial and two cancer cell lines. SonoVue[™] MBs were chosen since they are commonly used in the clinic as ultrasound contrast agents. The three cell lines were sonicated with identical US exposure conditions in the presence of MBs and the duration of model drug uptake was assessed. In addition, US pressure during sonication was varied to investigate its effect on the temporal window of uptake.

2. Materials and methods

2.1. Cell culture

MDA-MB-468 human breast cancer cells (ATCC[®] HTB-132[™], LGC Standards GmbH, Wesel, Germany) were maintained in high glucose – Dulbecco's Modified Eagle Medium (DMEM) supplemented with 10% fetal bovine serum (FBS; Sigma–Aldrich[®], St. Louis, MO, USA). 4T1 mouse breast cancer cells (ATCC[®] CRL-2539[™]) were grown in Roswell Park Memorial Institute (RPMI) 1640 medium supplemented with 10% FBS, and human umbilical vein endothelial cells (HUVEC; Lonza, Basel, Switzerland) were cultured in Endothelial Basal Medium-2 (EBM-2; Lonza) supplemented with Endothelial Growth Media-2 Microvascular complements (EGM[™]-2MV Single-Quots[™] kit; Lonza). HUVEC cells were used between passages 6–9. All cell lines were cultured in a humidified incubator at 37 °C and 5% CO₂, in standard cell culture flasks.

Two days prior to ultrasound experiments, cells were seeded into OptiCells[™] (Thermo Fisher Scientific Inc., Waltham, MA, USA). In the case of HUVEC cells, OptiCells[™] were coated with collagen I (Sigma–Aldrich[®]) prior to cell seeding to minimize US induced cell detachment.

2.2. Ultrasound contrast agent

SonoVue[™] (Bracco, Milan, Italy), a lipid shelled microbubble containing sulfur hexafluoride gas (SF₆), was used as a cavitation inducing agent in US experiments (Schneider, 1999). The MB suspension was prepared according to the manufacturer's protocol, yielding a mean bubble diameter of 2.5 μm, and a concentration ranging between 1 and 5 × 10⁸ microbubbles/mL. Before US experiments, 700 μL of fresh microbubbles was mixed with 9.5 mL medium, giving a suspension with a concentration of around 2 × 10⁷ MBs/mL, which was then injected into the OptiCell[™].

2.3. Chemicals

SYTOX[®] Green (Life Technologies[™] Europe BV, Bleiswijk, Netherlands; Excitation (Ex)/Emission (Em) wavelengths = 504/523 nm), a nucleic acid stain unable to penetrate into

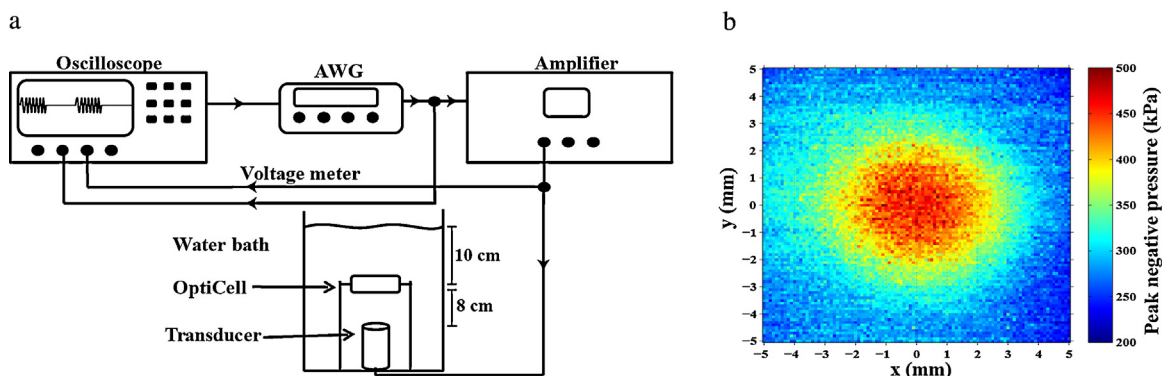


Fig. 1. (a) Schematic presentation of the ultrasound setup. (b) Horizontal XY plane of the ultrasound field measured at 80 mm perpendicular to the transducer. AWG = arbitrary waveform generator.

viable cells, was used as a marker for cell membrane permeability. SYTOX[®] Green's (MW ~ 600 Da) fluorescence intensity increases >500-fold upon binding DNA. These properties make it a model drug (Yudina et al., 2011; Derieppe et al., 2013) for US-induced uptake and nucleic acid binding, since most small chemotherapeutic drugs also depend on cellular internalization and DNA binding. In separate experiments, Hoechst 33342 (Sigma–Aldrich[®]; Ex/Em wavelength = 350/461 nm), a cell membrane permeable dye that binds to DNA, was used to detect all cells (i.e., permeabilized and non-permeabilized cells) in the field of view.

2.4. Ultrasound setup

Ultrasound experiments were performed with an unfocused mono-element piezoelectric US transducer (Precision Acoustics, Dorchester, UK) with a 20-mm diameter. The sinusoidal signal (1.5 MHz) was generated by an arbitrary waveform generator (Agilent Technologies, Santa Clara, CA, USA). An oscilloscope (Agilent Technologies) triggered the arbitrary waveform generator to generate a pulsed waveform (Fig. 1a), which was fed to an amplifier (K.M.P. Electronics, Bédoin, France). The US set-up was calibrated using a 125 μ m glass fiber hydrophone (Precision Acoustics) by measuring the ultrasound pressure field 80 mm from the transducer (Fig. 1b). Hydrophone measurements also showed that the two OptiCell membranes attenuated less than 2% of the US beam. The water surface was 10 cm above the OptiCell to prevent the buildup of standing waves.

In pilot experiments, duty cycle (1, 2.5, 5, 10, 15 and 20%), pressure (150–600 kPa peak negative pressure (PNP)), sonication time (5–30 s), and MB concentration (3×10^6 – 2×10^7 MBs/mL) were varied to find a balance between model drug uptake and cell viability. The acoustic parameters used in this study were frequency = 1.5 MHz, pulse repetition frequency = 1 kHz, duty cycle = 10%, total sonication time = 5 s, 100 μ s pulse duration (150 cycles), peak negative pressure = 400, 500 and 600 kPa. Similar pressure levels can be reached with diagnostic ultrasound imaging instruments, and are used in the clinic (Szabo, 2004). These pressure levels are much lower than those used for tumor ablation protocols with High Intensity Focused Ultrasound (HIFU).

2.5. Experimental protocol

To investigate the temporal window of SYTOX[®] Green uptake in different cell lines, 4T1, HUVEC and MDA-MB-468 cells were exposed to 500 kPa US. MDA-MB-468 cells were also exposed to

400 and 600 kPa US to investigate the effect of pressure on the temporal window. In each OptiCell[™], six regions were sonicated. The center of the regions was marked to identify the center of the US exposure area for optical microscopy (Fig. 2a), and bright field images were acquired prior to sonication. Each OptiCell[™] had two positive ($T = 0$; C and F, Fig. 2a) and two negative (no US; G and H, Fig. 2a) control regions. The remaining four regions (A, B, D and E, Fig. 2a) were sonicated at a certain time (–0.5, –1, –2, –3 or –24 h, Fig. 2b) prior to SYTOX[®] Green addition. OptiCells[™] were subconfluent at the time of the experiment and fresh medium mixed with MBs was added just before sonication.

The OptiCell[™] was placed in the 37 °C water bath with the cells on the upper wall. Subsequently, the four regions (A, B, D and E) were exposed to US within a 2 min time span and placed back in the incubator. At $T = 0$, medium in the OptiCell[™] was replaced with fresh medium, MBs and 2 μ M SYTOX[®] Green and the last two regions (C and F; $T = 0$) were exposed to US in the presence of the dye. Cells were incubated for 20 min with SYTOX[®] Green, after which bright field and fluorescent images (40 \times magnification, Eclipse TE2000-U, Nikon, Japan) were acquired of all areas (A–H, Fig. 2a). For all three cell lines, fluorescence microscopy images were analyzed and SYTOX[®] Green positive cells showing a fluorescent signal above a fixed threshold were counted automatically (ImageJ, NIH, Bethesda, MD, USA).

Cell counts in bright field images were performed only for MDA-MB-468 cells, which allowed calculations of the percentage of cells with model drug uptake. To confirm the accuracy of bright field cell counting of MDA-MB-468 cells in ImageJ, cells were counted in bright field images and fluorescence images after Hoechst 33342 staining in the same field of view.

2.6. Cell viability assay

MDA-MB-468 cell viability after US exposure in the presence of MBs was evaluated using a 3-(4,5-dimethylthiazol-2-yl)-2,5-diphenyltetrazolium bromide (MTT) colorimetric assay. Separate US experiments without dye were performed to measure cell viability, since SYTOX[®] Green is a DNA intercalating agent and therefore might compromise cell viability. For every OptiCell[™], three regions were sonicated and three regions were left untreated to serve as controls. Twenty-four hours after US exposure, the medium in the OptiCell[™] was replaced with fresh medium containing 1.2 mL MTT dye solution (CellTiter 96 Non-Radioactive Cell Proliferation Assay; Promega, Madison, WI, USA) and incubated for 1 h at 37 °C. Subsequently, 2 images of each region

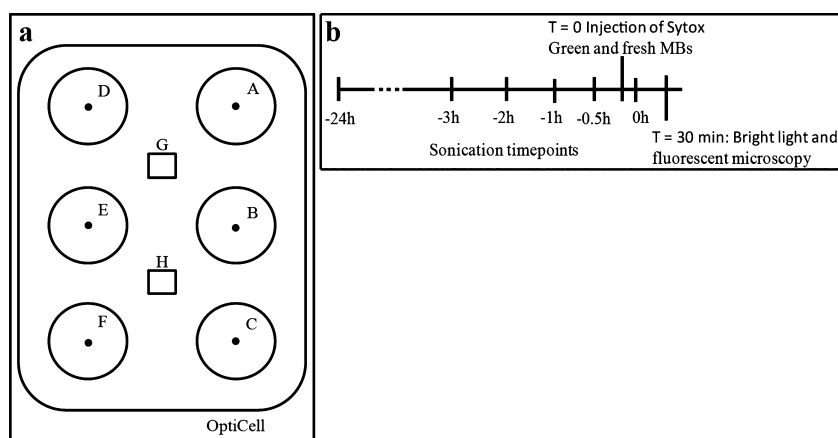


Fig. 2. (a) Schematic presentation of the OptiCell[™] and the sonication areas. Regions A, B, D and E were exposed to US before SYTOX[®] Green addition (at $T = -24$, -3 , -2 , -1 or -0.5 h). After adding SYTOX[®] Green, regions C and F were sonicated ($T = 0$; positive control). G and H are negative control areas. (b) Overview of different sonication time points in relation to addition of SYTOX[®] Green and fluorescence microscopy.

were acquired for cell counting. Pilot experiments demonstrated that 2 images of different quadrants of a (non-) sonicated region provide a reliable estimate for the total cell number. Next, the regions were cut out and placed in wells of a 24-well plate (Greiner Bio-One Alphen aan den Rijn, Netherlands) containing 300 μ L medium. After addition of 300 μ L solubilization/stop solution (Promega), the well plate was incubated for 1 h in the dark. Finally, the dye solution was homogenized by gentle pipetting and optical density was measured at 570 nm for formazan production, and 650 nm for background signal (Spectrostar Nano; BMG Labtech, Ortenberg, Germany). The MTT signals were normalized for the number of cells present after adding MTT dye.

2.7. Data analysis

Model drug uptake, *i.e.*, the number of SYTOX[®] Green positive cells, was counted for each time point (regions A, B, D and E). These numbers were normalized to the positive controls present in the same OptiCell[™] (regions C and F), which were set to 1. This allowed controlling for possible experimental differences, *e.g.*, variations in cell confluency.

Viability results were calculated as a percentage of the optical density produced by non-sonicated cells, which was set to 100% cell viability. In addition, the optical density was normalized for the number of cells in the circle in order to take minor US-induced cell detachment into account. One-way ANOVA followed by Tukey's multiple comparisons test (viability data) or Dunnet's multiple comparisons test (temporal window data) were performed using

GraphPad Prism version 6.00 for Windows (GraphPad Software; La Jolla, CA, USA), where $p < 0.05$ was considered to be statistically significant.

3. Results

3.1. Temporal window of SYTOX[®] Green uptake in MDA-MB-468 cells

At different time points after a single 500 kPa ultrasound exposure, SYTOX[®] Green was added to the medium of MDA-MB-468 cells, and the number of cells with uptake of the model drug was determined from fluorescent images. In Fig. 3, it can be observed that the number of cells with uptake was highest when cells were sonicated in the presence of the model drug in the medium, and decreased with increasing time between ultrasound exposure and addition of the model drug. Within cells that were sonicated 24 h prior to model drug addition, the number of cells with uptake was higher than non-sonicated cells.

3.2. The effect of ultrasound pressure on the temporal window in MDA-MB-468 cells

US pressures below 400 kPa resulted in dye uptake in less than 5% of total cells at $T = 0$, while pressures above 600 kPa resulted in major cell detachment (data not shown). Therefore, the results of the exposure of MDA-MB-468 cells to 400, 500 and 600 kPa US are shown in Fig. 4a, with cellular SYTOX[®] Green uptake as a function of time (Fig. 4b).

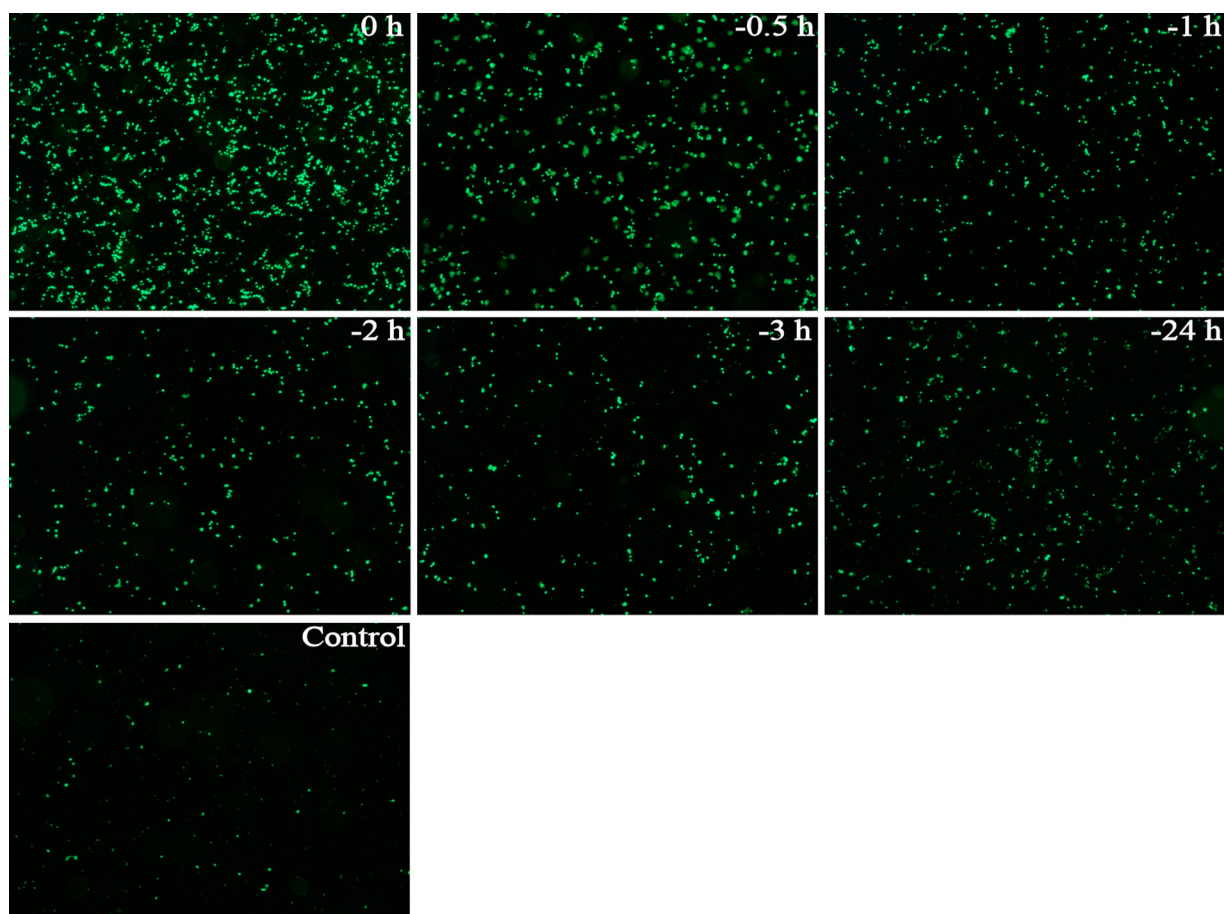


Fig. 3. Fluorescent images of SYTOX[®] Green positive MDA-MB-468 cells as a function of time between sonication at 500 kPa and dye addition. $T = 0$ h shows sonication in the presence of SYTOX[®] Green, the control image represents a non-sonicated area.

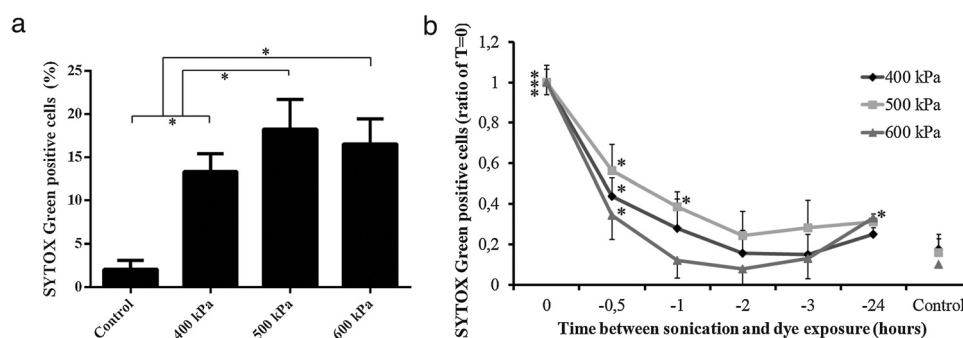


Fig. 4. (a) MDA-MB-468 cells with SYTOX[®] Green uptake as a % of total cells in the field of view after non-sonication or sonication at 400, 500, and 600 kPa. Cells were sonicated in the presence of SYTOX[®] Green ($T=0$). Significant differences are marked with asterisk * ($p < 0.05$). (b) Ratio of MDA-MB-468 cells with SYTOX[®] Green uptake at different time points between US exposure and dye addition. The number of SYTOX[®] Green positive cells at $T=0$ has been set to 1 for each US pressure independently. Values indicate mean \pm standard deviation ($N=4$). Significant differences with non-sonicated control cells are marked with asterisk * ($p < 0.05$).

For all acoustic pressures, the highest uptake was found at $T=0$. The maximum percentages of MDA-MB-468 cells with uptake were 13.3 ± 2.1 , 19.2 ± 3.5 and $16.6 \pm 2.9\%$ following sonication with 400, 500 and 600 kPa, respectively. In the analysis of the temporal window experiments, model drug uptake was normalized to the positive controls ($T=0$), which were set to 1. Cells exposed to 400 and 600 kPa US needed 1 h to return to uptake levels of non-sonicated cells, while cells exposed to 500 kPa US needed 2 h. There was a modest, though significant, increase in the number of SYTOX[®] Green positive cells 24 h post-exposure compared to previous time points after 600 kPa pressure. As mentioned, US exposure also induced cell detachment from the OptiCell[™] membrane. Sonication at 400, 500 and 600 kPa caused 18 ± 5 , 16 ± 6 and $31 \pm 6\%$ cell detachment, respectively. When cells that detached during sonication were seeded into normal cell culture flasks, they did not adhere or proliferate and were therefore considered non-viable (personal data, unpublished), similar to what was reported by Lu and Zhong (2005).

3.3. Cell viability of MDA-MB-468 cells following sonication

Viability of MDA-MB-468 cells exposed to US at 400, 500 and 600 kPa was measured using an MTT assay (Fig. 5a). Cells sonicated at 500 and 600 kPa US showed a significant reduction ($p < 0.05$) in cell viability. However, microscopy images illustrated US induced cell detachment after sonication, which impaired the MTT assay. Therefore, the MTT signal was normalized to the number of attached cells after sonication. The normalized MTT signal did not show reduced viability of the attached cells after US exposure.

3.4. Hoechst and SYTOX[®] Green co-administration

While the data of Fig. 4b was based solely on fluorescent images, the percentage of SYTOX[®] Green positive cells (Fig. 4a) was determined using both fluorescent and bright field images of the same field of view. In separate experiments, cells were treated with Hoechst 33342 to stain all the cells in the field of view. Hoechst stained cells could easily be counted using ImageJ, and this number was compared with a bright field cell count of the same field of view. This confirmed the accuracy of automated bright field cell count for MDA-MB-468 cells to be within 10% (data not shown). Analysis showed that the fluorescence intensity of SYTOX[®] Green positive cells was lower in presence of Hoechst than in its absence (Supplementary Fig. 1). Therefore, Hoechst staining was not used in standard temporal window experiments, since it was observed to compete with SYTOX[®] Green for DNA binding.

3.5. Temporal window of SYTOX[®] Green following sonication in three cell lines

In MDA-MB-468 cells, 500 kPa sonication resulted in the highest number of cells with SYTOX[®] Green uptake for all time points (Fig. 4). Therefore, this pressure was also used to assess the temporal window of model drug uptake in 4T1 and HUVEC cells. All three cell lines demonstrated a reduction in uptake with increasing time between sonication and model drug addition (Fig. 6). However, the cell lines exhibited different temporal window curves. The time-dependent uptake in 4T1 cells declined more slowly compared to other cell lines, with a 26% decrease of SYTOX[®]

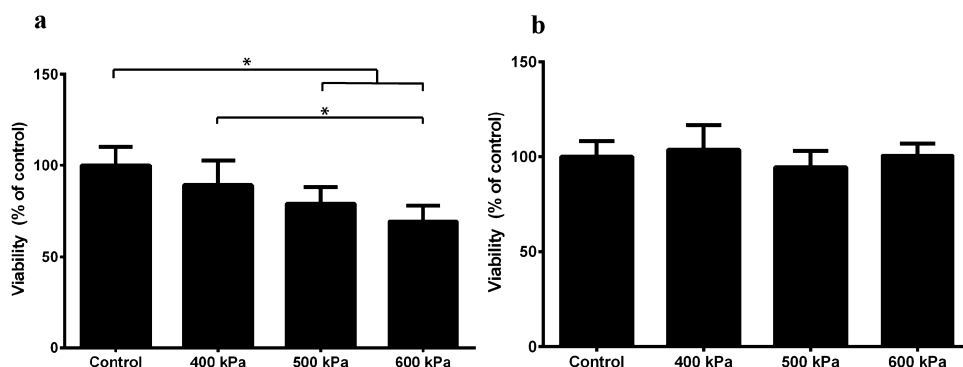


Fig. 5. (a) Viability of MDA-MB-468 cells as a function of US pressure. MTT signal for non-sonicated control cells was set at 100%. (b) Normalized viability of MDA-MB-468 cells as a function of US pressure. MTT signal was normalized for number of cells in two fields of view per (non-) sonicated region. Values indicate the sample mean \pm standard deviation ($N=6$). Significant differences are indicated with asterisk * ($p < 0.05$).

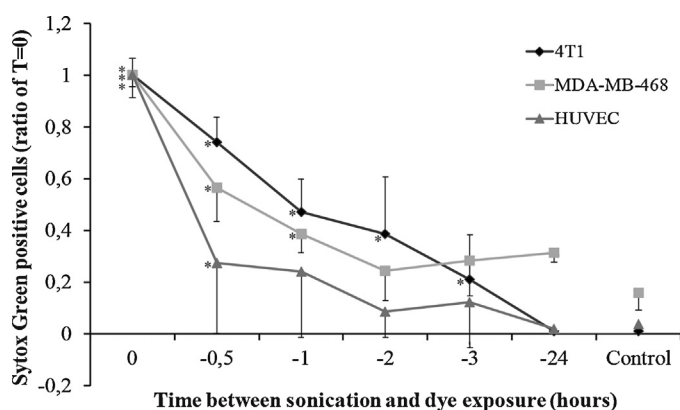


Fig. 6. Ratio of cells with SYTOX[®] Green uptake at different durations between US exposure and model drug addition. The positive control ($T=0$) has been set at 1. Values indicate mean \pm standard deviation ($N=4$). Significant differences with non-sonicated control cells are marked with asterisk * ($p < 0.05$).

Green positive cells at $T=-0.5$ h, as compared to 44 and 73% for MDA-MB-468 and HUVEC, respectively. Model drug uptake in 4T1 cells was significantly higher than in control cells up to 3 h after sonication, but returned to control level 24 h post-exposure. Within 2 h, the percentage of MDA-MB-468 cells with model drug uptake returned to that of control cells. For HUVEC cells, the percentage of cells with uptake was not significantly different anymore from that of non-sonicated cells 1 h post-sonication ($p=0.06$). Despite using collagen-coated OptiCells[™] for HUVEC experiments, US induced cell detachment resulted in high standard deviations in the HUVEC data. Due to cell morphology, bright field cell counts of 4T1 and HUVEC cells were not possible, excluding the option of measuring absolute uptake percentages in the temporal window experiments.

4. Discussion

The main goal of this study was to investigate the duration of enhanced membrane permeability, *i.e.*, temporal window, following identical US exposures in different cell lines. As mentioned before, depending on the route of administration, microbubbles can be in direct contact with endothelial or cancer cells. Therefore, these studies were conducted in one endothelial (HUVEC) and two cancer cell lines (MDA-MB-468 and 4T1). In all three cell lines, the number of cells with SYTOX[®] Green uptake was maximal when sonication was performed in the presence of the model drug. The number of cells with uptake decreased with increasing time between sonication and addition of model drug. Uptake in HUVEC and MDA-MB-468 cells returned to the control value after 1 and 2 h post-sonication, respectively, whereas this took more than 3 h for 4T1 cells. If a similar duration of membrane permeability could be found in a 3D *in vitro* model or *in vivo*, this would have implications for future treatment protocols. For example, a single ultrasound exposure could be advantageous throughout an IV drug infusion.

Under our experimental conditions, the measured durations of membrane permeability after US exposure are much longer (*i.e.*, 1–3 h) than the seconds or minutes described previously for similar model drugs (Van Wamel et al., 2006; Schlicher et al., 2006) and shorter than 24 h reported by Yudina et al. (2011) for the same model drug as the present study. These large differences in temporal windows described in the literature can be explained partly by the different cell lines used, but perhaps more importantly by the different US setups, *e.g.*, microbubbles used and US parameters applied, or the way of measuring uptake. US parameters used in this study were selected in line with literature on sonoporation (Lentacker et al., 2014). However, US pressure was

limited in our study to 400–600 kPa due to insufficient model drug uptake and cell detachment. In our results, MDA-MB-468 cells exposed to 400, 500 and 600 kPa US demonstrated slightly different temporal window curves, with the percentage of permeabilized cells decreasing to baseline within 1–2 h after sonication. Interestingly, at $T=-24$ h, the number of MDA-MB-468 cells with model drug uptake increased significantly compared to previous time points for 600 kPa sonicated cells. This rise in permeable cells 24 h post-sonication may be related to a delayed apoptotic response to US exposure. Indeed, sonication can trigger a cascade of events in subcellular organelles, eventually leading to apoptosis (Zhong et al., 2013). Cell membrane pores increase in size with increasing acoustic pressure, resulting in cell death when pore size exceeds the cell's capacity to reseal (Qiu et al., 2010). Although in this study cell detachment increased with increasing acoustic pressure, a reduced viability was not observed for adherent cells after sonication.

As mentioned above, the great disparities can also be explained by the various ways of measuring uptake of model drugs. For example, Van Wamel et al. (2006) determined the temporal window using fluorescent microscopy, counting the percentage of 500 cells with model drug uptake. On the other hand, Schlicher et al. (2006) assessed the temporal window based on the intracellular calcein concentration, measured by flow cytometry, and normalized to the extracellular concentration. Yudina et al. (2011) measured the mean fluorescence intensity of cells with model drug uptake in microscopy images. The latter method can be prone to a bias due to a few death cells with high fluorescence intensity in the field of view.

This relatively long temporal window for the three cell lines found here raises the question whether this can be ascribed to pore formation, endocytosis stimulation or another mechanism. Meijering et al. (2009) suggested that small model drugs (*i.e.*, <4.4 kDa) are predominantly internalized through pores immediately after sonoporation. Previous studies reported that US induced membrane pores reseal in seconds (Hu et al., 2013; Zhou et al., 2009) to minutes (Schlicher et al., 2006; Pan et al., 2005). To the best of our knowledge, there are no reports on the duration of endocytosis up-regulation after US exposure. An experimental design that allows discriminating between uptake through pores and uptake by endocytosis could be used to further elucidate the mechanism of uptake of these (model) drugs at the different time points.

The present study has a few limitations. For the data analysis of MTT and permeability assays, it would have been desirable to obtain the total cell counts using Hoechst staining. However, SYTOX[®] Green fluorescence decreased when Hoechst was co-administered. While SYTOX[®] Green has little base selectivity, Hoechst has a preference for double stranded AT-rich DNA (Portugal and Waring, 1988). As a result, the decrease in SYTOX[®] Green fluorescence intensity observed can reflect a competition of both intercalating fluorescence probes to the same DNA sites. These findings ruled out the possibility of using Hoechst in all experiments to obtain the total cell counts. Therefore, total cell counts were derived only by bright field microscopy images. A second limitation is the concentration of microbubbles used in the present study, which is much higher than the *in vivo* concentration for contrast enhanced ultrasound. Although the concentration used in this study exceeds what is typically achieved using intravenous administration, intratumoral administration of MBs can lead to high local concentrations of MBs. Additionally, in the intravenous administration context, blood flow is a major parameter, which has to be considered to succeed in efficient drug delivery using sonoporation. However, flow was not taken into account in our *in vitro* setup, but may play a large role in the contact between microbubbles and cell membranes.

Further *in vivo* investigations are required to assess the temporal window in a tumor environment. Since most chemotherapeutic agents are administered by IV infusion, a long temporal window, as was found here, would be beneficial throughout the infusion after a single sonication. Otherwise, tumor tissues could be exposed to repeated sonoporation treatments to achieve an increased intratumoral therapeutic dose of chemotherapeutics (Zhao et al., 2011).

5. Conclusions

In this work, it is shown that microbubble-assisted US can be used for the internalization of model drugs by cells. US pressure affected the percentage of MDA-MB-468 cells taking up the model drug SYTOX[®] Green, as well as the temporal window of the membrane permeabilization. The temporal window of uptake after US exposure differed between cell lines, but was consistently in the order of 1–3 h for HUVEC, MDA-MB-468 and 4T1 cells.

Conflict of interest

The authors declare that they have no conflict of interest.

Acknowledgements

These studies were supported by the European Research Council (ERC) project 268906 “Sound Pharma”. The help of the Pharmaceutics department of the Utrecht University is acknowledged, in particular Joep van den Dikkenberg. The authors thank Jean-Michel Escoffre and Noboru Sasaki for their advice.

Appendix A. Supplementary data

Supplementary data associated with this article can be found, in the online version, at <http://dx.doi.org/10.1016/j.ijpharm.2014.12.013>.

References

- Cavalli, R., Bisazza, A., Lembo, D., 2013. Micro- and nanobubbles: a versatile non-viral platform for gene delivery. *Int. J. Pharm.* 456, 437–445.
- Deckers, R., Moonen, C.T.W., 2010. Ultrasound triggered image guided, local delivery. *J. Control. Release* 148, 25–33.
- Deng, C.X., Sieling, F., Pan, H., Cui, J., 2004. Ultrasound-induced cell membrane porosity. *Ultrasound Med. Biol.* 30, 519–526.
- Derieppe, M., Yudina, A., Lepetit-Coiffé, M., Denis de Senneville, B., Bos, C., Moonen, C.T.W., 2013. Real-time assessment of ultrasound-mediated drug delivery using fibered confocal fluorescence microscopy. *Mol. Imaging Biol.* 15, 3–11.
- Frenkel, V., 2008. Ultrasound mediated delivery of drugs and genes to solid tumors. *Adv. Drug Deliv. Rev.* 60, 1193–1208.
- Heath, C.H., Sorace, A., Knowles, J., Rosenthal, E., Hoyt, K., 2012. Microbubble therapy enhances anti-tumor properties of cisplatin and cetuximab *in vitro* and *in vivo*. *Otolaryngol. – Head Neck Surg.* 146, 938–945.
- Hernot, S., Klivanov, A.L., 2008. Microbubbles in ultrasound-triggered drug and gene delivery. *Adv. Drug Deliv. Rev.* 60, 1153–1166.
- Hu, Y., Wan, J.M.F., Hu, A.C.H., 2013. Membrane perforation and recovery dynamics in microbubble-mediated sonoporation. *Ultrasound Med. Biol.* 39, 2393–2405.
- Iwanaga, K., Tominaga, K., Yamamoto, K., Habu, M., Maeda, H., Akifusa, S., Tsujisawa, T., Okinaga, T., Fukuda, J., Nishihara, T., 2007. Local delivery system of cytotoxic agents to tumors by focused sonoporation. *Cancer Gene Ther.* 14, 354–363.
- Karshafian, R., Bevan, P.D., Williams, R., Samac, S., Burns, P.N., 2009. Sonoporation by ultrasound-activated microbubble contrast agents: effect of acoustic exposure parameters on cell membrane permeability and cell viability. *Ultrasound Med. Biol.* 35, 847–860.
- Keyhani, K., Guzmán, H.R., Parsons, A., Lewis, T.N., Prausnitz, M.R., 2001. Intracellular drug delivery using low-frequency ultrasound: quantification of molecular uptake and cell viability. *Pharm. Res.* 18, 1514–1520.
- Kooiman, K., Vos, H.J., Versluis, M., De Jong, N., 2014. Acoustic behavior of microbubbles and implications for drug delivery. *Adv. Drug Deliv. Rev.* 72, 28–48.
- Kotopoulos, S., Delalande, A., Popa, M., Mamaeva, V., Dimcevski, G., Gilja, O.H., Postema, M., Gjertsen, B.T., McCormack, E., 2014. Sonoporation-enhanced chemotherapy significantly reduces primary tumour burden in an orthotopic pancreatic cancer xenograft. *Mol. Imaging Biol.* 16, 53–62.
- Lamauskas, N., Novell, A., Escoffre, J.M., Venslauskas, M., Satkauskas, S., Bouakaz, A., 2013. Bleomycin delivery into cancer cells *in vitro* with ultrasound and SonoVue[®] or BR14[®] microbubbles. *J. Drug Target.* 21, 1–8.
- Lentacker, I., De Cock, I., Deckers, R., De Smedt, S.C., Moonen, C.T.W., 2014. Understanding ultrasound induced sonoporation: definitions and underlying mechanisms. *Adv. Drug Deliv. Rev.* 72, 49–64.
- Lu, X., Zhong, P., 2005. Ultrasound-induced cell detachment and gene transfection in adherent cells. *Acoust. Res. Lett. Online* 6, 195–200.
- Matsuo, M., Yamaguchi, K., Feril Jr., R.B., Endo, H., Ogawa, K., Tachibana, K., Nakayama, J., 2011. Synergistic inhibition of malignant melanoma proliferation by melphalan combined with ultrasound and microbubbles. *Ultrasound Sonochem.* 18, 1218–1224.
- Mehier-Humbert, S., Bettinger, T., Yan, F., Guy, R.H., 2005. Plasma membrane poration induced by ultrasound exposure: implication for drug delivery. *J. Control. Release* 104, 213–222.
- Mei, J., Cheng, Y., Song, Y., Yang, Y., Wang, F., Liu, Y., Wang, Z., 2009. Experimental study on targeted methotrexate delivery to the rabbit brain via magnetic resonance imaging-guided focused ultrasound. *J. Ultrasound Med.* 28, 871–880.
- Meijering, B.D.M., Juffermans, L.J.M., Van Wamel, A., Henning, R.H., Zuhorn, I.S., Emmer, M., Versteilen, A.M.G., Paulus, W.J., Van Gilst, W.H., Kooiman, K., De Jong, N., Musters, R.J.P., Deelman, L.E., Kamp, O., 2009. Ultrasound and microbubble-targeted delivery of macromolecules is regulated by induction of endocytosis and pore formation. *Circ. Res.* 104, 679–687.
- Pan, H., Zhou, Y., Izadnegahdar, O., Cui, J., Deng, C.X., 2005. Study of sonoporation dynamics affected by ultrasound duty cycle. *Ultrasound Med. Biol.* 31, 849–856.
- Portugal, J., Waring, M.J., 1988. Assignment of DNA binding sites for 4′,6-diamidine-2-phenylindole and bisbenzimidazole (Hoechst 33258). A comparative footprinting study. *Biochim. Biophys. Acta BBA – Gene Struct. Exp.* 949, 158–168.
- Qiu, Y., Luo, Y., Zhang, Y., Cui, W., Zhang, D., Wu, J., Zhang, J., Tu, J., 2010. The correlation between acoustic cavitation and sonoporation involved in ultrasound-mediated DNA transfection with polyethylenimine (PEI) *in vitro*. *J. Control. Release* 145, 40–48.
- Sasaki, N., Kudo, N., Nakamura, K., Lim, S.Y., Murakami, M., Kumara, W.R.B., Tamura, Y., Ohta, H., Yamasaki, M., Takiguchi, M., 2012. Activation of microbubbles by short-pulsed ultrasound enhances the cytotoxic effect of cis-diamminedichloroplatinum(II) in a canine thyroid adenocarcinoma cell line *in vitro*. *Ultrasound Med. Biol.* 38, 109–118.
- Schlicher, R.K., Radhakrishna, H., Tolentino, T.P., Apkarian, R.P., Zarnitsyn, V., Prausnitz, M.R., 2006. Mechanism of intracellular delivery by acoustic cavitation. *Ultrasound Med. Biol.* 32, 915–924.
- Schneider, M., 1999. Characteristics of SonoVue[™]. *Echocardiography* 16, 743–746.
- Szabo, T.L., 2004. Ultrasound-induced bioeffects. In: Szabo, T.L. (Ed.), *Diagnostic Ultrasound Imaging: Inside Out*. Academic Press, pp. 489–516.
- Van Wamel, A., Kooiman, K., Harteveld, M., Emeer, M., Ten Cate, F.J., Versluis, M., De Jong, N., 2006. Vibrating microbubbles poking individual cells: drug transfer into cells via sonoporation. *J. Control. Release* 112, 149–155.
- Watanabe, Y., Aoi, A., Horie, S., Tomita, N., Mori, X., Morikawa, H., Matsumura, Y., Vassaux, G., Kodama, T., 2008. Low-intensity ultrasound and microbubbles enhance the antitumor effect of cisplatin. *Cancer Sci.* 99, 2525–2531.
- Yudina, A., Lepetit-Coiffé, M., Moonen, C.T.W., 2011. Evaluation of the temporal window for drug delivery following ultrasound-mediated membrane permeability enhancement. *Mol. Imaging Biol.* 13, 239–249.
- Zhao, Y.Z., Luo, Y.K., Lu, C.T., Xu, J.F., Tang, J., Zhang, M., Zhang, Y., Liang, H.D., 2008. Phospholipids-based microbubbles sonoporation pore size and reseal of cell membrane cultured *in vitro*. *J. Drug Target.* 16, 18–25.
- Zhao, Y.Z., Lu, C.T., Zhou, Z.C., Jin, Z., Zhang, L., Sun, C.Z., Xu, Y.Y., Gao, H.S., Tian, J.L., Gao, F.H., Tang, Q.Q., Li, W., Xiang, Q., Li, X.K., Li, W.F., 2011. Enhancing chemotherapeutic drug inhibition on tumor growth by ultrasound: an *in vivo* experiment. *J. Drug Target.* 19, 154–160.
- Zhong, W., Chen, X., Jiang, P., Wan, J.M.F., Qin, P., Yu, A.C.H., 2013. Induction of endoplasmic reticulum stress by sonoporation: linkage to mitochondria-mediated apoptosis initiation. *Ultrasound Med. Biol.* 39, 2382–2392.
- Zhou, Y., Kumon, R.E., Cui, J., Deng, C.X., 2009. The size of sonoporation pores on the cell membrane. *Ultrasound Med. Biol.* 35, 1756–1760.
- Zhou, Y., Yang, K., Cui, J., Deng, C.X., 2012. Controlled permeation of cell membrane by single bubble acoustic cavitation. *J. Control. Release* 157, 103–111.